

# Spin nematic order in multiple-spin exchange models on the triangular lattice

Tsutomu Momoi,<sup>1</sup> Philippe Sindzingre,<sup>2</sup> and Kenn Kubo<sup>3</sup>

<sup>1</sup>*Condensed Matter Theory Laboratory, RIKEN, Wako, Saitama 351-0198, Japan*

<sup>2</sup>*Laboratoire de Physique Théorique de la Matière Condensée, UMR 7600 of CNRS, Université P. et M. Curie, case 121, 4 Place Jussieu, 75252 Paris Cedex, France*

<sup>3</sup>*Department of Physics and Mathematics, Aoyama Gakuin University, 5-10-1 Fuchinobe, Sagamiara, Kanagawa 229-8558, Japan*

(Dated: November 30, 2011)

We figure out that the ground state of a multiple-spin exchange model applicable to thin films of solid  $^3\text{He}$  possesses an octahedral spin nematic order. In the presence of magnetic field, it is deformed into an antiferro-quadrupolar order in the perpendicular spin plane, in which lattice  $Z_3$  rotational symmetry is also broken. Furthermore, this system shows a narrow magnetization plateau at half,  $m/m_{\text{sat}} = 1/2$ , which resembles recent magnetization measurement [H. Nema *et al.*, Phys. Rev. Lett. **102**, 075301 (2009)].

PACS numbers: 75.10.Jm, 75.40.Cx

Frustrated quantum antiferromagnets have long been a subject of active research [1], since Anderson[2] suggested that a spin-1/2 Heisenberg antiferromagnet on the triangular lattice would have a gapless spin liquid ground state named as resonating-valence-bond (RVB) state. Recent experimental studies of quasi-two-dimensional compounds, such as solid  $^3\text{He}$  films absorbed on graphite [3–5], the organic Mott insulator [6]  $\kappa$ -(BEDT-TTF) $_2\text{Cu}_2(\text{CN})_3$  and the transition metal chloride  $\text{Cs}_2\text{CuCl}_4$  [7], have further prompted theoretical research of quantum spin liquid and competing exotic orders in triangular lattice antiferromagnets [8–14].

Among these, solid  $^3\text{He}$  films offer a perfect realization of a spin-1/2 triangular lattice. They contain a unique character in spin exchange interactions. The nearest-neighbor interaction is *ferromagnetic* (FM) and competes with antiferromagnetic (AF) multiple-spin cyclic exchange [15, 16]. As such,  $^3\text{He}$  on graphite belongs to a new class of quasi-two dimensional systems to exhibit “frustrated ferromagnetism” [17, 18]. It is also unique in the possibility of tuning the ratio of the competing interactions continuously by varying the density of  $^3\text{He}$  atoms. An additional strong motivation for understanding this system comes from the fact that, for a range of densities bordering on ferromagnetism, spins in solid  $^3\text{He}$  films exhibit anomalous double-peak structure in specific heat [4] with gapless excitations [5].

The effective Hamiltonian for nuclear magnetism of  $^3\text{He}$  thin films is given by the  $S = 1/2$  multiple-spin exchange (MSE) model on the triangular lattice [15]. The Hamiltonian containing up to six-spin exchanges and ap-

plied field is written as

$$H_{\text{eff}} = J \sum_{\langle i,j \rangle} P_2 + J_4 \sum_{\text{diamond}} (P_4 + P_4^{-1}) - J_5 \sum_{\text{triangle}} (P_5 + P_5^{-1}) + J_6 \sum_{\text{hexagon}} (P_6 + P_6^{-1}) - h \sum_i S_i^z, \quad (1)$$

where  $P_n$  denotes the cyclic permutation operator of  $n$  spins. The summations in front of the permutation operators run over all minimal  $n$  spin clusters. The first and the second summations, for example, run over all pairs of nearest neighbors and all four-spin diamond clusters, respectively. In solid  $^3\text{He}$  on graphite, the effective two-spin coupling  $J$  is negative (FM) and the other couplings  $J_n$  ( $n = 4, 5, 6$ ) are positive. Experimental estimates suggest that two-spin and four-spin exchange interactions are dominant, but five-spin and six-spin interactions are also not small [16]. We set  $J = -2$  and the ratio  $J_6/J_5 = 2$  throughout this letter.

Magnetism induced by multiple-spin exchange on the triangular lattice has been studied mostly in the  $J$ - $J_4$  model [9–14], which contains two-spin and four-spin exchanges. When FM  $J$  strongly competes with AF  $J_4$ , it was found that, in a finite range bordering on ferromagnetism, three magnon bound states become the most stable magnetic particles, giving rise to an octupolar ordered phase in applied magnetic field [14]. However the nature of the ground state in the absence of magnetic field was not identified in this regime. When four-spin exchange  $J_4$  is dominant, exact diagonalization analysis concluded a quantum disordered state with a large spin gap [12, 13]. The strong  $J_4$  also supports a wide magnetization plateau at half of saturation ( $m/m_{\text{sat}} = 1/2$ ), which originates from the appearance of four-sublattice spin density wave with *uud* structure [9, 11, 12].

In this letter, we study  $S = 1/2$  MSE model on the

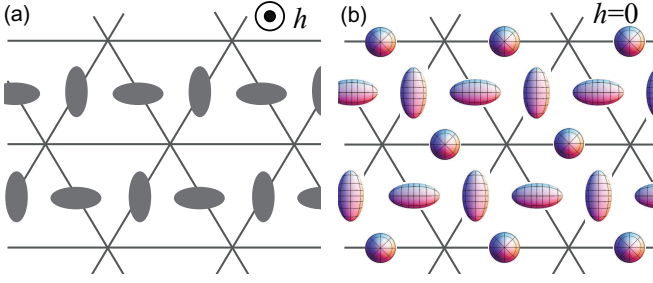


FIG. 1: Director configurations in spin nematic order in  $S = 1/2$  MSE model on the triangular lattice. Ellipses on bonds represent nematic-directors. In the applied field (a), only spin transverse components are depicted and there are also induced uniform dipole moments on sites. At zero field (b), three types of director vectors are orthogonal to each other.

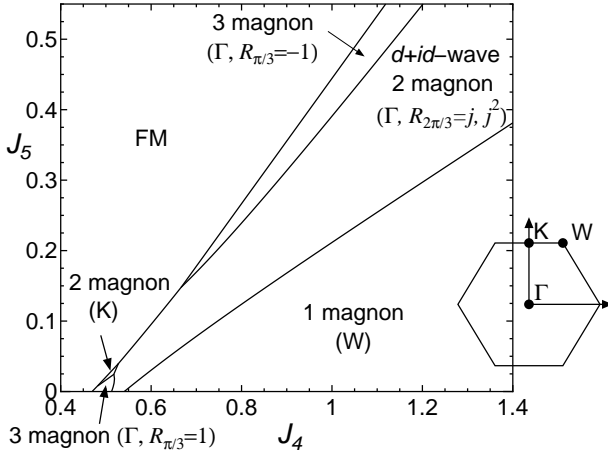


FIG. 2: Magnon instabilities to the fully polarized state at the saturation field. Parameters are set as  $J = -2$  and  $J_6 = 2J_5$ . The wave vectors in the Brillouin zone ( $\Gamma$ ,  $K$ ,  $W$ , defined in the inset) and some space symmetries are shown. FM denotes the stable ferromagnetic phase.

triangular lattice containing up to six-spin exchange couplings [Eq. (1)], which is directly applicable to solid  $^3\text{He}$  films. Inclusion of these multiple spin exchanges helps us to identify that the ground state is an octahedral spin nematic state [Fig. 1(b)], which has both liquid-like character and antiferro-quadrupolar orders on bonds. In applied field, this spin state is continuously deformed into a spin nematic state with antiferro-quadrupolar order [Fig. 1(a)], where lattice  $Z_3$  rotational symmetry is also broken. This state is understood as condensation of  $d + id$ -wave two magnon bound states.

The occurrence of this spin state may indeed be most easily understood from the channel of magnon instability at saturation field. As shown in Fig. 2, magnon pairs form stable bound states in a wide range near the FM phase boundary. As previously seen [19–21], con-

densation of bound magnon pairs leads to a spin nematic state [22], which has quadrupolar order in the perpendicular component to the applied field and breaks the  $U(1)$  symmetry of the Hamiltonian. In the triangular lattice  $J$ - $J_4$  model (i.e.  $J_5 = J_6 = 0$ ), instabilities given by two magnon bound states [20] and three magnon bound states [14] are competing. Inclusion of five and six-spin exchange interaction removes this competition, making the  $d_{x^2-y^2} + id_{xy}$ -wave two magnon instability most dominant in a wide parameter range near FM phase boundary, as shown in Fig. 2. The  $d + id$ -wave magnon pairing operators are given by  $Q_+ = \sum_i (S_i^- S_{i+e_1}^- + j S_i^- S_{i+e_2}^- + j^2 S_i^- S_{i+e_1-e_2}^-)$  and its complex conjugate  $Q_-$ , where  $j = \exp(i2\pi/3)$  and  $e_1 = (1, 0)$ ,  $e_2 = (1/2, \sqrt{3}/2)$ . The parameter set [16] estimated in the 4/7 phase of two-dimensional (2D) solid  $^3\text{He}$  also belongs to this instability region.

The  $d + id$ -wave bound magnon pairs  $Q_{\pm}|\text{FP}\rangle$ , where  $|\text{FP}\rangle$  denotes the fully polarized state, are degenerate with chiral degrees of freedom as the eigenvalues to the space rotation by  $2\pi/3$  are  $R_{2\pi/3} = j, j^2$ . In such a case, strong repulsion between different species of bosons can induce density imbalance between the condensates of two species, breaking additional chiral  $Z_2$  symmetry.

To identify the nature of symmetry breaking, we have performed numerical exact diagonalization of Eq. (1) for clusters up to  $N = 36$  spins. For parameter sets in the two-magnon instability regime, the special stability of lowest energy states in even  $S$  sector at large magnetization (high  $S$  states), as seen in Fig. 4(b), signals the formation of bound magnon pairs with repulsive interactions, which leads to jumps by  $|\Delta S| = 2$  in the magnetization process as shown Fig. 3 and points to spin nematic ordering in the perpendicular spins [21].

From the analysis of irreducible representations (irreps) and quasi-degeneracy of these low-lying states, we conclude to non-chiral spin nematic ordering. A quasi three-fold degeneracy is observed in low-lying states in the even spin  $S$  sector (for  $S < m_s - 2$ ), instead of the two-fold degeneracy expected for the chiral nematic. It indicates that bound magnon pairs with different chiralities condense with the same density and an additional  $Z_3$  symmetry is broken.

The order parameter of this non-chiral nematic state is identified as

$$\mathcal{O}_{U(1)} = Q_+ - Q_- = i\sqrt{3} \sum_i (S_i^- S_{i+e_1}^- - S_i^- S_{i+e_2}^-), \quad (2)$$

by expansion of the coherent state  $\exp[-\lambda \mathcal{O}_{U(1)}]|\text{FP}\rangle$  into irreps, which gives the numerically observed irreps. The required low-lying states for this order are listed in Table I(a). Note that space rotational  $Z_3$  symmetry is broken in this order parameter, corresponding to the choice of two bonds out of three. A schematic figure of nematic-directors for this state is depicted in Fig. 1(a). The

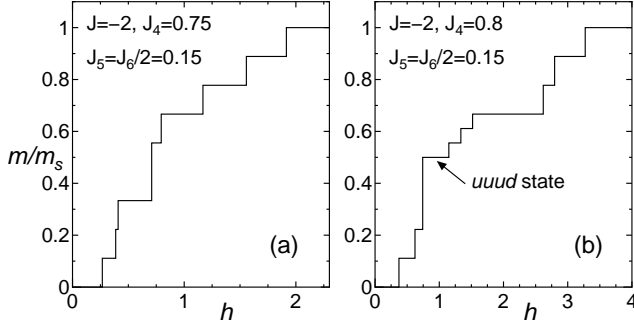


FIG. 3: Magnetization process  $m/m_s$  of the MSE model for  $N = 36$  spin cluster. The exchange parameters are  $J = -2$ ,  $J_5 = \frac{1}{2}J_6 = 0.15$  with (a)  $J_4 = 0.75$  and (b)  $J_4 = 0.8$ . Jumps of  $|\Delta m| = 2$ , corresponding to spin nematic order, are clearly visible. In (b), a narrow plateau structure appears at  $m/m_s = 1/2$ .

(a) $h > 0$ , $U(1)$ symmetric case						
$m$	$m_s - 2$	$m_s - 4n$	$m_s - 2(2n + 1)$			
Irreps	$\Gamma_3$	$\Gamma_1, \Gamma_3$	$\Gamma_2, \Gamma_3$			
(b) $h = 0$ , $SU(2)$ symmetric case						
$S$	0	2	3	4	5	6
Irreps	$\Gamma_2$	$\Gamma_3$	$\Gamma_1$	$\Gamma_2, \Gamma_3$	$\Gamma_3$	$\Gamma_1, \Gamma_2, \Gamma_3$

TABLE I: Irreps of low lying states in each total spin  $S$  (magnetization  $m$ ) sector, needed for antiferro-quadrupolar ordering, (a) in applied field and (b) at zero field. The symbols are defined as  $\Gamma_1 \equiv (R_{2\pi/3} = 1, R_\pi = 1, \sigma = 1)$ ,  $\Gamma_2 \equiv (R_{2\pi/3} = 1, R_\pi = 1, \sigma = -1)$ ,  $\Gamma_3 \equiv (R_{2\pi/3} = j, j^2, R_\pi = 1)$ , and all of them have the wave vector  $\mathbf{k} = (0, 0)$ .

ground state manifold has spin  $U(1)/Z_2$  symmetry and space  $Z_3$  symmetry.

In the absence of magnetic field,  $SU(2)$  symmetry is restored and the signature of  $SU(2)$  symmetry breaking is the existence of an “Anderson tower” of quasidegenerate joint states (QDJS) belonging to different spin sectors which form the  $N = \infty$  ground state with energies scaled as  $E_{QDJS} \sim \frac{S(S+1)}{N}$  and are well separated (at finite  $N$ ) from the lowest magnon excitations (scaled as  $\sim 1/\sqrt{N}$ ). The energy spectrum around  $S = 0$  is shown in Fig. 4(a) for the parameter set  $J = -2$ ,  $J_4 = 0.5$ ,  $J_5 = J_6 = 0$ . A similar spectrum structure is also found for finite  $J_5$ , for example in  $J = -2$ ,  $J_4 = 0.8$ ,  $J_5 = \frac{1}{2}J_6 = 0.15$ . The spin  $S = 1$  sector has high energy, which excludes conventional spin ordering. Comparing irreps of the low energy states with those expected for various possible spin structures, we found that these states perfectly match with the Anderson tower of a spin nematic state with three sets of orthogonal directors, whose order parameter is given by

$$\mathcal{O}_{SU(2)} = \sum_i \{Q_i^{xx}(\mathbf{e}_1) + Q_i^{yy}(\mathbf{e}_2) + Q_i^{zz}(\mathbf{e}_1 - \mathbf{e}_2)\}, \quad (3)$$

where  $Q_i^{\alpha\alpha}(\mathbf{r}) = S_i^\alpha S_{i+\mathbf{r}}^\alpha - \frac{1}{3}\langle \mathbf{S}_i \cdot \mathbf{S}_{i+\mathbf{r}} \rangle$ .

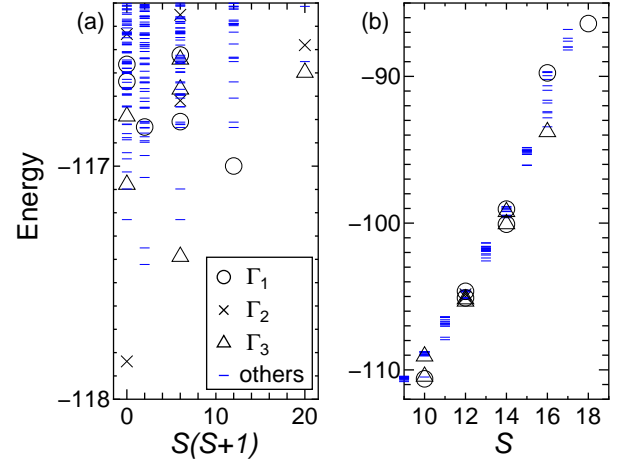


FIG. 4: (Color online) Energy spectrum of the MSE model for  $N = 36$  spin cluster with (a)  $J = -2$ ,  $J_4 = 0.5$ ,  $J_5 = J_6 = 0$  near the singlet ( $S = 0$ ) and (b)  $J = -2$ ,  $J_4 = 1$ ,  $J_5 = \frac{1}{2}J_6 = 0.3$  near the saturation ( $S = 18$ ). The symbols  $\Gamma_1$ ,  $\Gamma_2$ , and  $\Gamma_3$  are defined in Table I.

This order parameter has octahedral spin symmetry  $O$ , if one combines spin transformations with the space group  $C_{6v}$  of the triangular lattice. To obtain irreps specific to this spin state, one may decompose the irreps  $D^S$  of  $SU(2)$  into irreps of  $O$  in each spin  $S$  sector [23] and remove irreps odd under  $\pi$  rotation ( $C_4^2$ ), i.e. the three dimensional irreps  $F_1$  and  $F_2$ , which should be absent as the nematic order parameter is invariant under  $C_4^2$  (since directors are headless). This allows projection only on  $A_1$ ,  $A_2$ , and  $E$ . For  $N = 36$  spins,  $A_1$ ,  $A_2$ , and  $E$  map onto  $\Gamma_1$ ,  $\Gamma_2$ , and  $\Gamma_3$  of  $C_{6v}$ , respectively ( $\Gamma_\mu$  are defined in Table I). The irreps for  $N = 36$  in each spin  $S$  sector are shown in Table I(b), which agrees well with symmetries of QDJSs found in Fig. 4(a). The mapping of  $A_1$  and  $A_2$  to  $\Gamma_1$  and  $\Gamma_2$  may interchange depending on the number of spins  $N$ . (Note that, only the relative symmetries between QDJSs are important for constructing symmetry broken states). With this assignment, irreps around  $S = 0$  smoothly connect with those of low-lying states determined by the two-magnon instability at saturation field. While the dynamics of the order parameter of a non-collinear Néel is that of a symmetric top, which has  $2S + 1$  states in each total spin  $S$  and magnetization  $m$  sector, here the ground state manifold has spin  $SU(2)/D_2$  symmetry and so the Anderson tower has  $S/2 + 1$  [ $(S - 1)/2$ ] states for even (odd)  $S$  sector, the same as a symmetric top which are even under  $\pi$  rotations around the principal axes.

In applied field, two orthogonal nematic directors become perpendicular to the field and the other doesn't have any order in the perpendicular plane, leading to the space  $Z_3$  symmetry breaking. The QDJSs around  $S = 0$  smoothly merge with the series of low-lying states at high

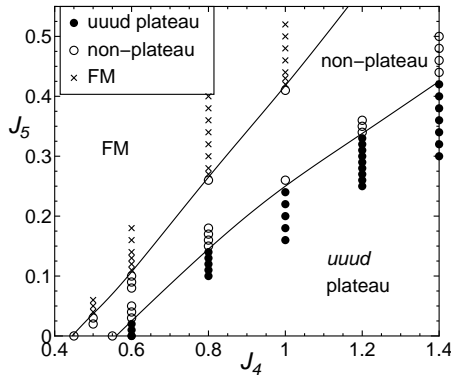


FIG. 5: Phase diagram of the MSE model in  $m/m_{\text{sat}} = 1/2$ . The exchange parameters are set as  $J = -2$  and  $J_6 = 2J_5$ . Spin nematic phase spreads over most of the “non-plateau” region.

magnetization. Thus the octahedral spin nematic state at zero field is continuously deformed into the spin nematic state under the field.

The order parameter  $\mathcal{O}_{SU(2)}$  has the same spin symmetry as the antiferro-quadrupolar (AFQ) state discussed in the triangular lattice  $S = 1$  bilinear-biquadratic model [24, 25]. The irreps of QDJSs for the  $S = 1$  AFQ state, obtained from the decomposition of the wave function [26], are equivalent to the Anderson towers of the  $S = 1/2$  octahedral spin nematic state at zero field, through the mapping of the space groups. The difference is that the quadrupolar moments exist on bonds in the  $S = 1/2$  spin nematic state, whereas on sites in the  $S = 1$  AFQ state. In  $S = 1/2$  spin nematics,  $S = 1$  degrees of freedom are formed on bonds and moving around from bond to bond. The ground state is translationally invariant at any field, i.e., it doesn’t show any spin density wave, which is also different from the  $S = 1$  system [25]. Thus, the  $S = 1/2$  spin nematic state has a liquid-like character [21, 27] and cannot be decoupled into the site product state. On the other hand, the  $S = 1$  AFQ state is formed by the product of the quadrupolar moments localized on sites, having three sublattice structure with the wave vector  $\mathbf{k} = (4\pi/3, 0)$ .

The signature of spin nematic ordering in energy spectrum around  $S = 0$  was well detected in a wide parameter range  $J_5 \lesssim 0.2$  which covers the  $d + id$ -wave two-magnon instability region at saturation field slightly extending to the smaller  $J_4$  regime. In most of the region, the spin nematic state exists from zero magnetization to the saturation. Near  $J_5 = J_6 = 0$  regime, three magnon instability induces an octupolar order under magnetic field [14], but, at very low magnetization, the octahedral spin nematic order overcomes it, as shown in Fig. 4(a). For the  $J_5 > 0.3$  range, there is no more clear separation of QDJSs and also no signature of spin ordering.

Meanwhile, a wide magnetization plateau appears at

$m/m_s = 1/2$  due to the spin-gapped *uud* state in the strong  $J_4$  regime [9, 11, 12]. Recent magnetization measurement in 2D solid  $^3\text{He}$  observed a narrow plateau structure at  $m/m_s = 1/2$  [28]. To compare with this, we numerically obtained magnetic phase diagram in  $m/m_s = 1/2$  (Fig. 5). The *uud* phase is easily detected by the four-fold quasi degenerate low-energy states and a large energy gap above them. As shown in Fig. 5, the plateau phase spreads close to the FM phase boundary. Near its edge, the magnetization process has a very narrow plateau at  $m/m_s = 1/2$  [see Fig. 3(b)], which resembles the experimental observation. Even in this case, spin nematic phases appear in both low and high magnetization regime.

To summarize, strong competition between FM two-spin and AF multiple-spin interactions on the triangular lattice induces the octahedral spin nematic state with bond antiferro-quadrupolar order. This state is a strong candidate for explaining the anomalous magnetic behaviors experimentally observed in 2D solid  $^3\text{He}$ .

It is our pleasure to acknowledge stimulating discussions with Hiroshi Fukuyama, H. Ishimoto, M. Morishita, H. Nema, K. Penc, N. Shannon, and R. Shindou. Numerical calculations were conducted on RICC in RIKEN and at IDRIS. This work was supported by KAKENHI No. 17071011, No. 22014016, and No. 23540397.

- 
- [1] G. Misguich and C. Lhuillier, in *Frustrated spin systems*, edited by H. T. Diep (World Scientific, Singapore, 2004).
  - [2] P. W. Anderson, Mater. Res. Bull. **8**, 153 (1973).
  - [3] D. S. Greywall and P. A. Busch, Phys. Rev. Lett. **62**, 1868 (1989).
  - [4] K. Ishida, M. Morishita, K. Yawata, and H. Fukuyama, Phys. Rev. Lett. **79**, 3451 (1997).
  - [5] R. Masutomi, Y. Karaki, and H. Ishimoto, Phys. Rev. Lett. **92**, 025301 (2004).
  - [6] Y. Shimizu, K. Miyagawa, K. Kanoda, M. Maesato, and G. Saito, Phys. Rev. Lett. **91**, 107001 (2003).
  - [7] R. Coldea, D. A. Tennant, A. M. Tsvelik, and Z. Tylczynski, Phys. Rev. Lett. **86**, 1335 (2001).
  - [8] See for example, L. Balents, Nature **464**, 199 (2010) and references therein.
  - [9] K. Kubo and T. Momoi, Z. Phys. B **103**, 485 (1997).
  - [10] T. Momoi, K. Kubo, and K. Niki, Phys. Rev. Lett. **79**, 2081 (1997).
  - [11] T. Momoi, H. Sakamoto, and K. Kubo, Phys. Rev. B **59**, 9491 (1999).
  - [12] G. Misguich, B. Bernu, C. Lhuillier, and C. Waldtmann, Phys. Rev. Lett. **81**, 1098 (1998).
  - [13] G. Misguich, C. Lhuillier, B. Bernu, and C. Waldtmann, Phys. Rev. B **60**, 1064 (1999).
  - [14] T. Momoi, P. Sindzingre, and N. Shannon, Phys. Rev. Lett. **97**, 257204 (2006).
  - [15] M. Roger, Phys. Rev. Lett. **64**, 297 (1990).
  - [16] E. Collin *et al.*, Phys. Rev. Lett. **86**, 2447 (2001).
  - [17] H. Kageyama *et al.*, J. Phys. Soc. Jpn. **74**, 1702 (2005).
  - [18] E. Kaul *et al.*, J. Magn. Magn. Matt. **272–276(II)**, 922

- (2004).
- [19] A. V. Chubukov, Phys. Rev. B **44**, 4693 (1991).
  - [20] T. Momoi and N. Shannon, Prog. Theor. Phys. Suppl. **159**, 72 (2005).
  - [21] N. Shannon, T. Momoi, and P. Sindzingre, Phys. Rev. Lett. **96**, 027213 (2006).
  - [22] A. F. Andreev and I. A. Grishchuk, Sov. Phys. JETP **60**, 267 (1984).
  - [23] M. Hamermesh, *Group theory and its application to physical problems* (Dover Publications, 1989)
  - [24] H. Tsunetsugu and M. Arikawa, J. Phys. Soc. Jpn. **75**, 083701 (2006)
  - [25] A. Läuchli, F. Mila, and K. Penc, Phys. Rev. Lett. **97**, 087205 (2006).
  - [26] K. Penc and A. Läuchli, in *Introduction to Frustrated Magnetism*, edited by C. Lacroix *et al.* (Springer, 2011).
  - [27] R. Shindou and T. Momoi, Phys. Rev. B **80**, 064410 (2009).
  - [28] H. Nema, A. Yamaguchi, T. Hayakawa, and H. Ishimoto, Phys. Rev. Lett. **102**, 075301 (2009).